Broadband Microwave Absorber based on End-loading Folded-Dipole Array

Yumei Chang [1] and Yung L. Chow [2]

[1] College of Electronic and Optical Engineering
Nanjing University of Posts & Telecommunications, 210023 Nanjing, China
changym@njupt.edu.cn

[2] Department of Electrical and Computer Engineering, University of Waterloo, Waterloo, ON, Canada N2L3G1
ylchow@maxwell.uwaterloo.ca

Abstract ─ Microwave absorbers have been widely used in electromagnetic compatibility, radar absorbing material and cloaking etc., and therefore attract much attention in recent years. In this work, a microwave absorber based on an array of receiving folded-dipoles with a grounded air spacer is proposed. The cell of the absorber can be seen as a three resonators in tandem formed by dipole-mode and stub-modes of the receiving folded dipole and the grounded spacer with thickness of $\lambda/4$, i.e., an equivalent three-pole filter. Based on the equivalent circuit, the impedance matching during a wide frequency range can be achieved. Moreover, to verify the proposed technique, a prototype of dual-polarized absorber is fabricated and measured. A little variation between the simulation and measurement results are observed, however, the relative bandwidth can still reach up to 105%. In addition, compared with other absorbers constructed with metal and lumped elements, the proposed absorber has a high ratio of *bandwidth/thickness*, which is around 8.5 and be with dual-polarizations.

Index Terms ─ Electromagnetic shielding, equivalent circuit, folded dipole array, microwave absorber.

I. INTRODUCTION

Electromagnetic absorber have been used in many areas, such as Radar Absorbing Material (RAM) for improving the radar performance (by reducing interfering reflections from other objects) or radar camouflages [1], measurements of electromagnetic compatibility (EMC) and measurements of antenna radiation pattern in anechoic chambers etc.

The classical Salisbury screen invented by Salisbury in 1952 is one type of well-known absorbers, which is constructed with a resistive sheet of 377 Ω /sq. and a backing ground plane at $\lambda/4$ away [2]; and gives a perfectly zero reflection at the resonance. Others like Dallenbach layers loaded with high impedance surfaces, circuit analogue RAMs, magnetic absorbers, and lossy frequency selective surfaces has been investigated [3] - [7]; however, most of their relative bandwidths are not wide – substantially less than 100%.

Usually, to furtherly enhance the bandwidth, multi-layer structure is the primary choice. A capacitive circuit absorber with three layers in [8], which replaces the band-stop resonating frequency selective surfaces (FSS) with low-pass capacitive circuit analog absorber (CA absorber) that gives a very wide bandwidth of 4 GHz to 24 GHz. Some other examples use optimization method like Genetic Algorithm (GA) to find the optimal layer thickness so as to achieve a maximum bandwidth [9]. Unfortunately, although the bandwidth can be made very wide, the absorber is bulky, difficult to fine adjust on the layers and therefore expensive. In [10], double square loop and dipole with lumped resistors are used to form the absorber, which can achieve better performance at the absorption band; but the bandwidth is not very wide. Other structures like 3-D periodic absorber invented by Shen's group [11]. In their work, a periodic structure of 3-D geometry with lump elements is introduced between the ground plane and the top resistive/capacitive layer. A microwave absorber of 100% bandwidth was achieved and the performance of absorption under oblique incidence were stable at the range of $\theta = 0^{o}$~30^{o}. However, it is some kind of difficult to assemble for its 3-D geometry and the amount of soldering work involved.

Generally, in most publications, absorbers based on periodic cells are considered as independent microwave circuits or an extensive application of FSS. However, in our previous work [12-13], the design of an absorber starts with a *receiving antenna*. The most difference from the absorber and the traditional receiving antenna is that the incident wave received by the former ones is mostly dissipated, while by the latter ones is transmitted to the next level. Therefore, the absorber based on periodic cells can be seen as a special application of receiving antenna array. In [14], Lin etc. also proposed a broadband absorber of single-polarization with the receiving antenna concept.

Submitted On: May 16, 2018
Accepted On: May 12, 2019

In this work, a novel broadband absorber constructed with a top-loading folded-dipole array is proposed. The measured results show a small deviation from the simulations, that the measured relative bandwidth is 105% approximately, which is less than our expectation. The reasons might be the wide band has reached the frequency limit of the measuring system. Besides, the parasitic effects of the surface mounted resistor also contribute to the frequency deviation. For further demonstration, we compare the performances of this absorber with others in the literatures above, and find that the proposed absorber can achieve wide bandwidth but with small thickness.

II. EQUIVALENT CIRCUITS & DESIGNS

A. Equivalent circuit of the absorber cell based on folded dipole

As mentioned above, an absorber is more like a receiving antenna array, while the receiving EM wave dissipated other than transmitted to the receiver, as shown in [12]. In this work, the folded dipole array receive the incident wave and then dissipate on the load at the center and end of the dipole. Each cell of the absorber is equivalent to a square waveguide (with electric or magnetic walls) loaded across with a folded-dipole with resistor R_L, and followed by a $\lambda/4$ spacer to a ground plane. Figure 1 gives the corresponding equivalent circuit , while the upper R_u of the stub mode comes from the optional loading R_s at the end of each stub of the ($\lambda/4$) folded dipole, with $R_u = Z_0^2/R_s$; the lower R_d is similar to R_u. The equivalent circuit is composed of three resonators, i.e., a parallel-circuit resonator (of the stub mode of the folding), a series-circuit resonator (of the mode of a standard dipole) and then a parallel-circuit resonator (of the unit cell stub of spacer and ground below the folded-dipole). The resonators in tandem, parallel to series to parallel, perform as standard filter.

Nevertheless, the equivalent circuit of the unit cell in Fig. 1 does not precisely describe the characteristics of folded-dipole absorber; this is because a) the fringe fields have been neglected, e.g., the field effect of the short end of the folded-dipole. More importantly, b) the Z_M from the mutual impedances of all adjacent folded-dipoles outside the unit cell is tedious to derive analytically. Therefore, based on the equivalent circuit, one can move S_{11} loops in Smith chart analytically, such as *up*, *down*, *left*, *right*, and *changing loop sizes*. The goal of the moves above is to fit the multi-loop locus of S_{11} within the -10 dB circle at the center of the Smith chart as long a length as possible; and therefore make the bandwidth as wide as possible.

Table 1 lists the links of the physical parameters to the impedance and reflections of the absorber surface; following these links, a regular folded dipole with initial settings of $D = 4a_r$, $a_l = a_r = 0.15$ mm, $l_u = l_d = l = 25$mm and $R_A = 600$ ohm can be improved to have a wide bandwidth of 99.1%.

Table 1 Parameter adjustments and its theoretical basis

Parameter Adjustments	Theoretical Basis and Dffects
$D\uparrow$	$C_r\uparrow$and $L_r\uparrow$, then $Q\downarrow$, and then wider bandwidth
a_r	To achieve wide bandwidth, it is better to have $\frac{dX_T}{df} + \frac{dB_t}{df} = 0$ in a wide band.
K	When D is fixed, a proper value of a_r and K can be found.
$l_u<l$ & $l_d<l$	Off-tuning the resonances, to get a maximum length of frequency locus running within the -10 dB circle
R_A	To suppresses the high current and therefore the lowers the reflections S11 of the spurious resonances to below -10 dB over a wide band.

B. A practical wideband dual-polarized absorber

A dual-polarized folded dipole array for practical use is a little more complicated than a singly polarized one. Therefore, for the dual polarized folded dipole array as a practically wideband absorber, three further adjustments may be needed and given below.

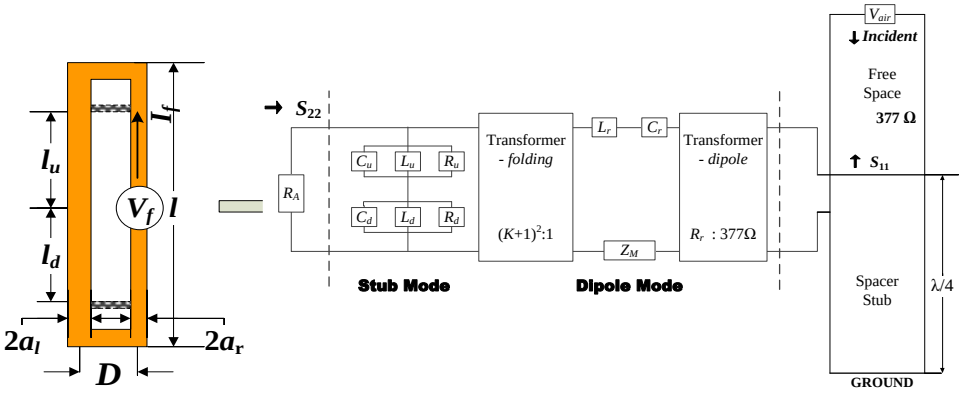

Fig. 1. Equivalent circuit of a unit cell on a folded-dipole array absorber.

(a) Increasing the dipole length to get off-tuning

By *top-loading* the dipole with triangles at the sides of each end of the dipole as shown in Fig. 2, the dipole length l is effectively made longer but still within the unit cell. Obviously, the length $2l_u$ twin-strip stubs is shorter than the dipole l, and with a suitable *off tuning* between the stub and dipole modes, one can get a wider band, as listed in Table 1.

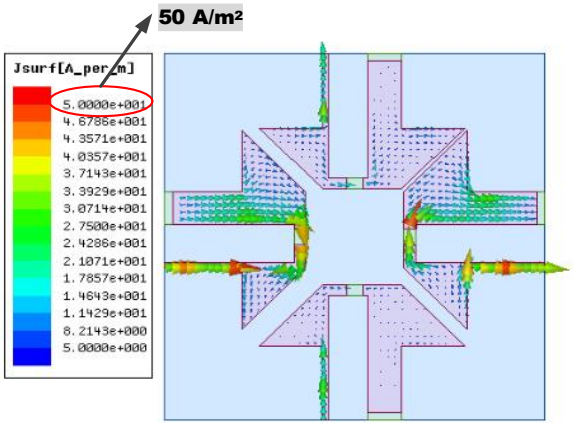

(a) R_s = 60 ohm, J_{max} = 50 A/m

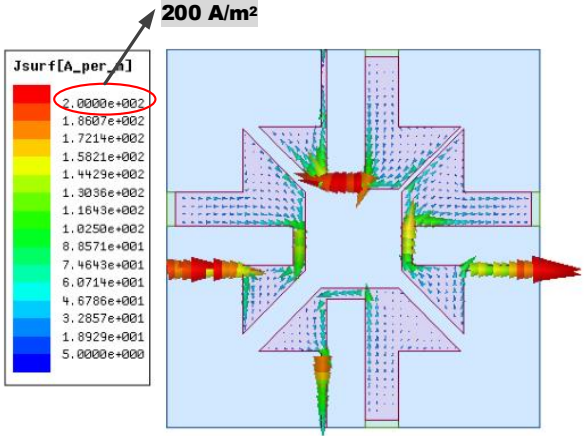

(b) R_s = 0, J_{max} = 200 A/m

Fig. 2. Current distributions at f = 7.2 GHz for the two cases.

(b) Adding Rs to each end of the folded dipole to suppress spurious mode

The closeness of the dipole ends means high capacitance between them, which might produce an extraneous mode of narrow band of high S_{11}. The extraneous mode can bring strong current flowing across the short circuits of the opposite folded dipoles as bridges from the left to the right. However, the strong current can be suppressed by inserting a resistor of the R_s. Figure 2 also shows the actual current flow of suppression before and after the insertion of R_s. Figures 3 (a) and 3 (b) show the corresponding elimination of the spurious S_{11}, in the Smith chart and in linear plots. Meanwhile, R_s is about 60 Ω, which is substantially smaller than the characteristic Z_0 of the twin-strip at about 200 Ω; as a result, the presence R_s does not significantly affect the characteristic of the open circuit resonator.

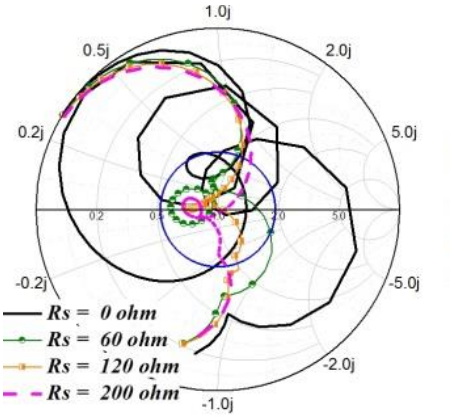

(a) S_{11} in Smith chart

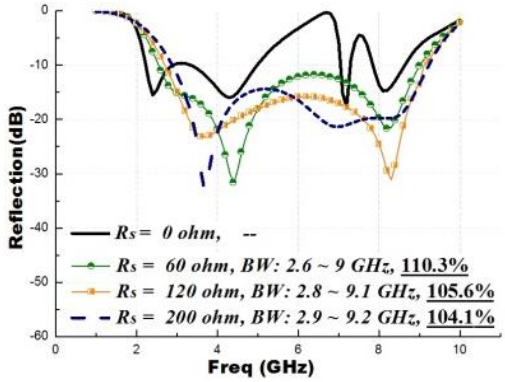

(b) Linear S_{11} vs. f

Fig. 3. Adding *Rs* to illuminate the spurious mode.

(c) Flipping thin dielectric slab on top of the air spacer

Generally, the folded dipole is usually printed on the top of the dielectric slab; however, to protect the metal parts of the absorber, one can flip the normal dielectric slab, and so that the folded dipoles are printed at the bottom of the dielectric slab as shown in Fig. 2. The flipping of the thin Teflon slab change the mutual couplings a little between the dipole ends, and therefore changes the excitation of the spurious mode as well. This means that the resistance R_s at the end of the folded dipole may be adjusted slightly to get the best suppression of the spurious mode and the final optimized bandwidth of the absorber. When t = 0.5 mm, Fig. 4 then shows the final S_{11} and bandwidths of the absorber, at the flipped case and the normal cases. Although the bandwidth improvement is not very significant, the flipping moves the printed folded dipoles behind the dielectric slab; and the move does provide some mechanical protect to the folded dipoles against possible mechanical damages,

e.g., scratches causing an open circuit to a folded dipole in the array. Additionally, the move can also protect the metal parts from oxidation and other chemical damages in some extent. Most importantly, the final bandwidth of the flipped case can reach up to 120%, i.e., a ratio of 4:1 between the upper and lower frequency limits.

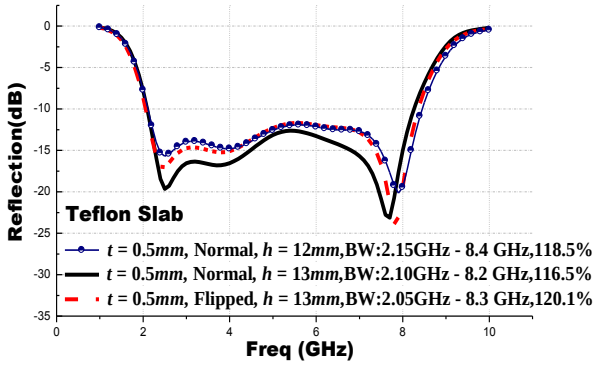

Fig. 4. Comparison of reflections of the absorber surface with optimized parameters in different cases, while a_l =0.2mm, a_r = 1.2mm, D = 4.2mm, b_f = 4.5mm, l_t = 20mm, a_e = 0.4mm, R_A = 300 ohm and R_s = 80 ohm.

III. RESULTS AND DISCUSSIONS

A. Experimental validation and discussions

To validate the final designs at Fig. 4 of the folded dipole absorber with flipped and normal slabs, we fabricated two prototypes with same array size (300mm * 300mm) but with different total thicknesses h. They both consist of 11*10 folded dipole elements as in Fig. 5. By using plastic screws via the slab to the ground, one can easily adjust the distance between them, which is also the thickness of the spacer. For practical engineering, however, the foam spacer may still be necessary because of its mechanical stability. The measurement setup is composed of two wideband horn antennas positioned on an arch support, with operating range of the horns from 2 GHz to 18 GHz.

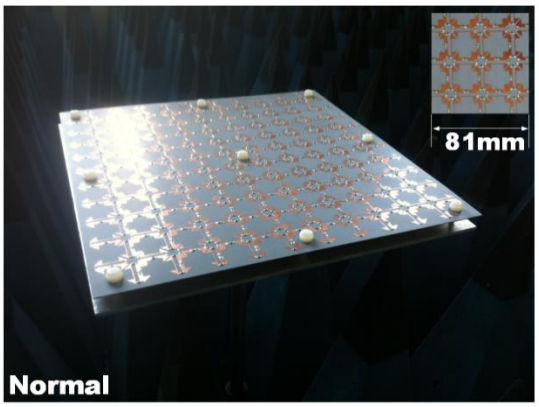

(a) Folded dipoles in Normal position

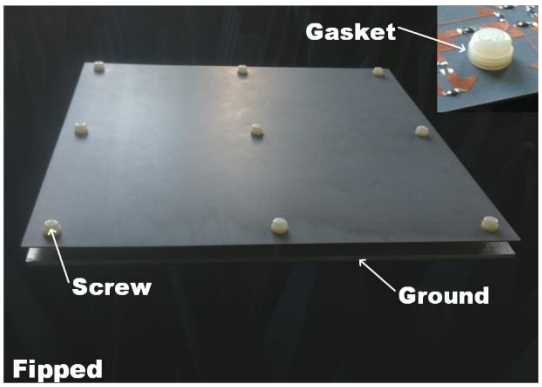

(b) Flipped folded dipole array

Fig. 5. Prototype of the absorber surface made of top-triangle-loaded folded dipole.

Figure 6 then shows the measured and simulated reflection coefficients of the four absorbers with similar physical parameters, except that the position and the thicknesses of the slab.

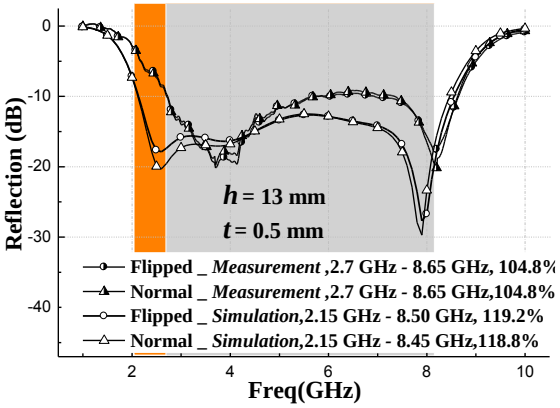

(a) t = 0.5 mm

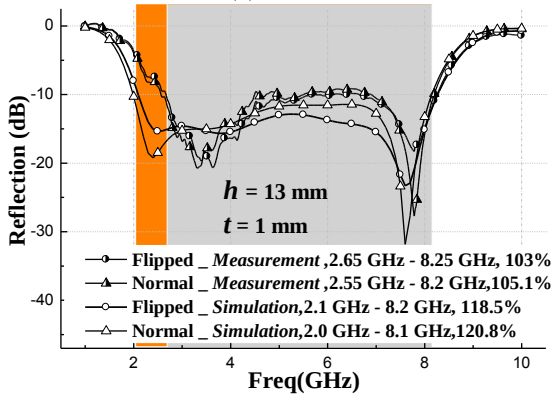

(b) t = 1 mm

Fig. 6. Comparison of the reflections between simulation and measurement for the cases of slab with different, while a_l = 0.2 mm, a_r = 1.2 mm, D = 4.2mm, b_f = 4.5 mm, l_t = 20 mm, a_e = 0.4 mm, R_A = 310 ohm and R_s = 82 ohm.

From Fig. 6, one can find that the measured result has a small deviation from the simulated ones at the lower frequency part, which the lower limit of the frequency band moves from 2 GHz to 2.6 GHz, and therefore leads to a decrease of the relative bandwidth, i.e., from 120% to 104%. The reasons could be as the follows: 1) the simulated bandwidth of the dipole is from 2 GHz to 8.3 GHz, in which the lower bounder is reaching the measurement limit of the horn antenna. This means that the feeding horn is operating at the right to its frequency limit, and minor error would happen at the limit; 2) the parasitic effects appeared on the Surface-mount resistor. The prototype measured in this work contains 11*10 cells, and each cell has eight resistors. For the consideration of cost, we apply normal surface-mount resistors to the cell, which might bring parasitic inductive reluctance at higher frequencies, and lead to a frequency deviation to the right. Actually, to decrease the parasitic effects, the author tried to lower the center frequency of the absorber, but still bound to the measurement system. However, if we did not consider too much on the cost, the results would agree well with the simulation results.

Figure 6 also indicates that the differences in S_{11} between absorbers made of normal slab and flipped ones is little. One can see that, the bandwidths for both cases are almost same, which means that the effects of flipping is very less. However, in practical engineering, the flipped structure of Fig. 5 (b) might be better in preventing from the unexpected mechanical damages to the printed folded dipoles.

B. S_{11} of the dual-polarized surface under oblique incidences of TE and TM Modes

Figures 7 (a) and 7 (b) give the calculated S_{11} vs. f for the case of (slab thickness) t = 1 mm, in the TE and TM incidence directions respectively. Figures 7 (a) and 7 (b) also show the angular stability of S_{11} vs. f curves of the dual-polarization absorber surface of the folded dipole array. Angular stability represents the effects of the oblique incident waves on the bandwidth of the absorber. For instance, when the direction of the incident wave θ is under 30° (from the normal direction of the absorber), the -10 dB bandwidth can be above 100% for both the TE and TM waves; the angular stability may be said to be good. As the angle θ becomes 45°, the reflections become larger but can still be under -7dB (absorption of 80%) during a wide band, one can still consider the angular stability as reasonably good.

C. *Discussions*

Table 2 lists the comparisons between our work and others published in recent years. Note that the that the *fractional bandwidth* of the absorber usually refers to $FB=(f_h-f_l)/f_0$, while f_h and f_l denote the upper and lower frequency limits of $|S_{11}|\leqslant$-10dB (the absorption A = (1-$|S_{11}|^2$)*100%, -10dB of $|S_{11}|$can get an absorption of 90%, which is good enough for most applications). From Table 2, one can find that, with the techniques of lossy FSS or metal FSS with lumped elements, the widest bandwidth is 117% in Ref. [7], but the thickness is larger and then lead to a lower value of Q, which is only five. In our work, the relative bandwidth of our proposed folded-dipole absorber can reach up to 120% in simulation, and 105% in measurement. Besides, by comparing the value of Q of each absorber in Table 2, one can also find that, the proposed absorber in this work has shown a good performance.

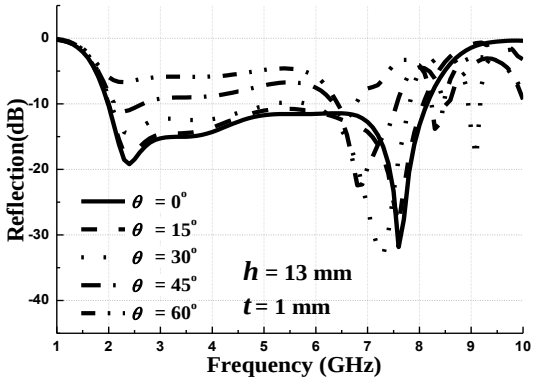

(a) TE wave

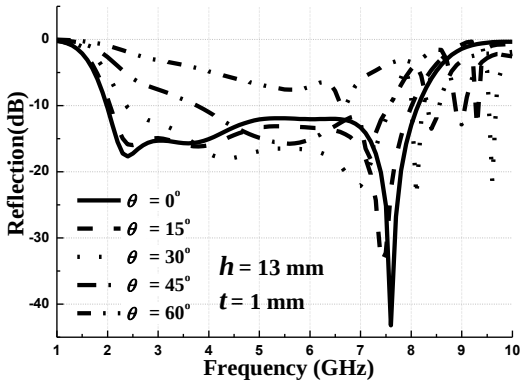

(b) TM wave

Fig. 7. S_{11} of the absorber surface under oblique incident waves, while the oblique angle is ranging from 0° to 60°.

Table 2: Comparison of numerical results of different absorber surfaces in the literature

Absorbing Surface Type	Type	Spacers	Total Thickness (d)	$f_L \sim f_H$ (GHz) ($BW = \frac{2(f_H - f_L)}{f_H + f_L} \times 100\%$)	$Q = \Delta\lambda/d$ ($\Delta\lambda = \lambda_{max} - \lambda_{min}$)	Good Angular Stability
Ref. [4]	Shaped resistive sheet	Air	5.0 mm ($0.25\ \lambda_0^*$)	7 ~ 22 (BW=103.5%)	5.84	$0^o \sim 45^o$
Ref. [7]	Salisbury screen with resistive loading	Air	9.0 mm ($0.33\ \lambda_0$)	4.5 ~ 17.5 (BW=117%)	5.5	$0^o \sim 40^o$
Ref. [9]	Metal with lump resistors	FR4 substrate $\varepsilon_r = 4.4$	3.18 mm ($0.138\ \lambda_0$)	8 ~ 18 (BW=77%)	6.55	-
Ref. [10]	3-D geometry	$\varepsilon_r = 3$	20.0 mm ($0.22\ \lambda_0$)	1.5 ~ 5 (BW=107%)	7	$0^o \sim 30^o$
Our work	Metal with lump resistors	Teflon substrate ($\varepsilon_{r1} = 2.65$, $h_1 = 1$ mm) and foam ($\varepsilon_{r2} = 1.06$, $h_2 = 10$ mm)	11.0 mm ($0.19\ \lambda_0$)	2.05 ~ 8.3 (BW=120%)	10.02 (simulation)	$0^o \sim 45^o$

VI. CONCLUSION

A practical dual-polarized absorber surface with high ratio of *bandwidth/thickness* is proposed in this work, which is constructed in the form of a folded dipole array with a grounded spacer. Unlike the traditional understanding of the absorber made of lossy FSS, the proposed absorber surface in this work is considered as a receiving dipole array but dissipating the incident wave other than transmitting it to the receiver. To verify our proposal, we fabricated and measured two prototypes of the dual-polarized absorber with different thickness of the slab. The hardware experiments show that the bandwidth only reaches 105%, a small decrease from the simulation results, which is likely due to an error of the measuring system being pushed to its frequency limits, and the parasitic effects occurs at the surface-mounted resistors. However, the absorber in this work shows a quite good performance in $Q = \Delta\lambda/d$, which can be around 8.5.

In this work, all simulations are carried out through HFSS or CST; however, with the manipulations of the Smith chart guided by the equivalent circuit, the amount of computation might be quite small. This is in contrast with the amount of computation needed when optimization of the absorber surface is done solely by numerical means and over the whole structure in a one-off solution. It is reasonable to expect the computation and optimization of a device would speed up by making use of prior knowledge; to achieve this, the space mapping approach uses coarse segmentation; this paper uses equivalent circuit and Smith chart manipulations, and thus provides a good physical insight.

ACKNOWLEDGMENT

This work was financial supported by Natural Science Foundation of Jiangsu Province for Youth (Grant No. BK20160912), Natural Science Foundation of China for Youth (Grant No. 61701256) and NUPTSF (Grant No. NY215038).

REFERENCES

[1] W. H. Emerson, "Electromagnetic wave absorbers and anechoic chambers through the years," *IEEE Trans. Antennas Propagation*, vol. 23, no. 4, pp. 484-490, 1973.

[2] W. W. Salisbury, "Absorbent Body for Electromagnetic Waves," U.S. Patent 2-599-944, 10, 1952.

[3] B. Chambers and A. Tennant, "Active Dallenbach radar absorber," *IEEE Antennas and Propagation Society International Symposium*, pp. 381-384, 2006.

[4] F. Costa, A. Monorchia, and G. Manara, "Analysis and design of ultra-thin electromagnetic absorbers comprising resistively loaded high impedance surfaces," *IEEE Transaction on Antennas and Propagation*, vol. 58, no. 5, pp. 1551-1558, May 2010.

[5] C.-X. Yuan, Z.-X. Zhou, J. W. Zhang, X.-L. Xiang, Y. Feng, and H.-G. Sun, "Properties of propagation of electromagnetic wave in a multilayer radar-absorbing structure with plasma- and radar-absorbing material," *IEEE Transactions on Plasma Science*, vol. 39, no. 9, pp. 1768-1775, 2011.

[6] F. C. Seman, R. Cahill, V. F. Fusco, and G. Goussetis, "Design of a Salisbury screen absorber using frequency selective surfaces to improve bandwidth and angular stability performance," *IET Microwaves, Antennas & Propagation*, vol. 5, no. 2, pp. 149-156, 2011.

[7] H.-Y. Chen, H.-B. Zhang, and L.-J. Deng, "Design of an ultra-thin magnetic-type radar absorber embedded with FSS," *IEEE Antennas and Wireless Propagation Letters*, vol. 9, pp. 899-901, 2010.

[8] A. K. Zadeh and A. Karlsson, "Capacitive circuit method of fast and efficient design of wideband

radar absorbers," *IEEE Trans on Antennas and Propagation*, vol. 57, no. 8, pp. 2307-2314, 2009.
[9] B. Chambers and A. Tennant, "Optimized design of Jaumann radar absorbing materials using a genetic algorithm," *IEE Proceedings on Radar, Sonar and Navigation*, vol. 143, no. 1, pp. 23-30, 1996.
[10] J. Yang and Z. Shen, "A thin and broadband absorber using double-square loops," *IEEE Antennas and Wireless Propagation Letters*, vol. 6, pp. 388-391, 2007.
[11] A. K. Rashid, Z. Shen, and S. Aditya, "Wideband microwave absorber based on a two-dimensional periodic array of microstrip lines," *IEEE Transactions on Antennas and Propagation*, vol. 58, no. 12, pp. 3913-3922, 2010.
[12] Y. Chang, W. Che, and Y. L. Chow, "Dipole array absorbing surface made thin and wideband with inductive ground," *IEEE Asia Pacific Microwave Conference*, pp. 927-930, 2011.
[13] Y. Chang, W. Che, and Y. L. Chow, "Broadband dual-polarization microwave absorber based on broadside-folded dipole array with triangle-lattice cells," *IEEE Antennas and Wireless Propagation Letters*, vol. 13, pp. 1084-1087, 2014.
[14] X. Q. Lin, P. Mei, P. C. Zhang, et al., "Development of a resistor-loaded ultra-wideband absorber with antenna reciprocity," *IEEE Transactions on Antennas and Propagation*, vol. 64, no. 11, pp. 4910-4913, 2016.

Yumei Chang received the M.Sc. and Ph.D. degrees from the Nanjing University of Science and Technology (NUST), Nanjing, China, in 2009 and 2014. She is currently a Lecturer in Nanjing University of Posts and Telecommunications.

From September 2012 to February 2013, she was a Visiting Scholar in the Department of Electronic and Computer Engineering at University of Waterloo, Canada. She has authored or coauthored over 30 journal and conference papers. Her research interests include microwave absorbers, FSS and microwave/millimeter-wave devices.

Yung L. Chow received the Ph.D. degree from the University of Toronto, Toronto, ON, Canada, in 1965. From 1964 to 1966, he was with the National Radio Astronomy Observatory, where he designed the array configuration of the VLA of 27 25-m dishes of Socorro, NM. In 1966, he was with the University of Waterloo (UW), Waterloo, ON, Canada, where he was involved with numerical methods and simplification of electromagnetic theory for monolithic microwave integrated circuit (MMIC) designs. In 1996, he retired from UW and became a Professor with the City University of Hong Kong (CITYU), Hong Kong. In 2002, he returned to UW as Professor Emeritus. He has authored or coauthored over 320 journal and conference papers. He holds seven U.S. and Canadian patents.